ASIAN JOURNAL OF CIVIL ENGINEERING (BUILDING AND HOUSING) VOL. 11, NO. 5 (2010)
PAGES 645-661

NONLINEAR DYNAMIC ANALYSIS OF STRUCTURES UNDER NEAR-FAULT GROUND MOTIONS USING AN IMPROVED SCALING METHOD

A. Yahyaabadi* and M. Tehranizadeh
[a]Department of Civil Engineering, Amirkabir University of Technology, Tehran, Iran

ABSTRACT

Assessment of the seismic performance of a structure often requires conducting nonlinear dynamic analyses under a set of ground motion records scaled to a specific level of intensity using an appropriate scaling method. In this study to reduce the variability in the seismic demands, a seismic-intensity scaling index is developed through studying weaknesses and strengths of different scaling methods. Results of the incremental nonlinear dynamic analyses of generic frames with 3, 6, 9, 12 and 15 storey under 40 near-fault ground motions show that using root-mean-square value of pseudo spectral accelerations over effective period range of structures can considerably reduce the scatter in the dynamic responses particularly once higher modes and period elongation effects dominate the response. By using this scaling method, the amount of dispersion is nearly independent of the ductility demand level and the number of stories.

Keywords: Nonlinear dynamic analysis; near-fault ground motions; seismic demands; scaling method; dispersion

1. INTRODUCTION

The need for estimation the nonlinear engineering demand parameters of structures under severe earthquakes has led to the development of nonlinear analysis methods. One of these methods providing rigorous representation of structural behavior but also increasing requirements for modeling and complexity of the analysis is nonlinear time history analysis which can be used to determine the more detailed response history of a structure, particularly cyclic response, and degradation and damage measures for the members [1]. According to this structural analysis procedure in the current Iranian seismic design provisions the seismic demand parameters can be estimated using the results of the analyses under at least three scaled earthquake records. If three records are used, then the maximum value of the interested response parameter determined from analyses should be taken for design of the structure. The average of the response parameter can be used for design

* E-mail address of the corresponding author: A.yahyaabadi@aut.ac.ir (A. Yahyaabadi)

provided that at least seven scaled records are analyzed [2]. With the small number of ground motion records specified by the current Iranian seismic design provisions, the method used to scale the input records is of concern. The provisions require that time history pairs scaled as follows; the 5 percent-damped response spectra of each pair of accelerograms scaled to their maximum value shall be developed and combined, using the Square Root of the Sum of Squares (SRSS) method and then the motions shall be scaled such that the average value of their SRSS spectra is not less than 1.4 times the standard design-spectra for periods of 0.2T to 1.5T, where T is the fundamental period of vibration. In other words standard No. 2800 of Iran uses Peak Ground Acceleration (PGA) as the seismic scaling index to scale the records in accordance with the standard design-spectra at a specific site. Whereas previous research has demonstrated that scaling ground motions records based on the PGA introduces a large scatter in the analysis results [3,4].

Considering that the amount of confidence to the estimated median value of demands determined from nonlinear time history analyses is reversely proportional to the variability in the seismic demands, it can be said that the scatter in the demands is almost as important as the mean value of the demands in the seismic assessment of structures. It is worth noting that standard error of the estimated median demands is equal to $\sigma/\sqrt{n}$ where σ and n are the standard deviation of the results and the number of records that have been sampled respectively [5]. Therefore reasonable estimation of the median demand can be obtained using the small number of records provided that ground motions are scaled based on the parameter which can reduce the scatter in the dynamic responses. There are many papers that mention or explicitly address scaling of ordinary ground motion records. Miranda [4] found that using PGA to scale ground motions increases the scatter in the nonlinear acceleration demand spectra at long periods. Shome and Cornell [3] and Shome *et al.* [6] found that pseudo spectral acceleration at the structural fundamental period, $S_a(T_1)$, is strongly correlated with the seismic demands of SDOF and MDOF structures with two periods ($T_1=0.25$ and $T_1=1.05s$). However $S_a(T_1)$ has been the popular scaling method for ordinary earthquakes in the recent past, but it is a matter of debate whether this parameter is the appropriate scaling method for near-fault ground motions.

In near-fault records affected by forward directivity or fling step phenomena, most of the seismic energy from the rupture appears as a single coherent pulse-type motion. Ground motions having such a distinct pulse-like character arise generally at the beginning of the seismogram, and their effects tend to increase the long-period portion of the acceleration response spectrum [7]. Studies show that for this type of records, the maximum demand is a function of the ratio of the pulse period, T_P, to the fundamental period of the structure [8]. The scaling parameters which are responsible for the damage potential of ground motions should be able to adequately represent this peculiar characteristic of near-fault ground motions. Since the parameter of $S_a(T_1)$ does not account for enough information about the spectral shape of earthquake records may introduce a large scatter in the seismic demands when using as a basis for scaling near-fault pulse-like records [9]. In a study considering the efficiency of different intensity measure parameters for near-fault ground motions, Yang and coworker [10] have proposed two scaling parameters, namely, the Improved Effective Peak Acceleration (IEPA) and Improved Effective Peak Velocity (IEPV), based on the frequency characteristics of near-fault pulse-like ground motions and on the seismic responses of

bilinear single degree of freedom systems. However, these parameters present fairly good correlation with the seismic responses under impulsive ground motions, but for mixed ground motions including non-pulse ground motions could not be superior to corresponding conventional parameters, i.e. EPA and EPV as scaling parameters [10].

In this paper, with the objective of reducing the scatter in the dynamic responses of structures under near-fault pulse-like ground motions records, the efficiency of the PGA, EPA, EPV, IEPA, IEPV and $S_a(T_1)$ parameters as the seismic scaling index is studied and then based on the shortcomings of these parameters in representing the intensity of near-fault earthquakes a new scaling parameter is developed. Accordingly, the efficiency of the root-mean-square value of spectral accelerations, $(S_a)_{rms}$, in the range of effective periods of structures as the seismic scaling parameter is considered. To calculate the root-mean-square values, it is too important to determine the range of effective periods of structures. For this purpose different period ranges with respect to higher mode and period elongation effects at different ductility levels are evaluated and then the most effective period range is selected.

2. NEAR-FAULT GROUND MOTIONS DATABASE

Near-fault pulse-like ground motions are often characterized by intense velocity or displacement pulse with relatively long period that clearly distinguish them from typical far-field ground motions. The distinct characteristics of near-fault ground motions are originated from the forward directivity and fling step effects which had caused severe structural damage in recent major earthquakes [10], e.g. Northridge in 1994, Kobe in 1995, Chi-Chi, Taiwan in 1999 and Bam in 2003 and Wen-Chuan, China in 2008 etc.

Forward directivity occurs when the rupture propagation and the direction of slip on the fault are both toward a site. As the rupture front propagates away from the hypocenter and toward a site, energy is accumulated near the rupture front from each successive zone of slip along the fault. The wave front arrives as a large pulse of motion (a shock wave effect) that occurs at the beginning of the record [11]. Rupture-directivity effects can be presented both for strike-slip and dip-slip events. The pulse of motion is oriented perpendicular to the fault strike due to the radiation pattern of the shear dislocation on a causative fault [11].

Fling steps are permanent ground displacements due to the static deformation field of the earthquake, occurring over a discrete time interval of several seconds as the fault slip is developed [12]. The duration of these displacements is closely related to the characteristic slip time of a point on the fault, and there is evidence that this slip is rapid. Therefore, both shear-wave displacements as in forward directivity, and static displacement as in fling step emerge as the pulse [8]. As a word of caution, fling step displacements always occur in the direction of fault slip, and therefore are not strongly coupled with the aforementioned dynamic displacements referred to as the rupture-directivity pulse [13].

Owing to the forward directivity and fling step effects, pulse motions emerge in near-fault grounds motions and strongly affect the structural responses. As a result the dynamic responses of structures would have a large variability unless appropriate method is used in scaling the input ground motions. Therefore, the focus of this study is on a database of 40 pulse-like earthquake records is compiled from records that exhibit intense velocity pulses

for studying in this paper. 35 numbers of these records are selected from those which have been identified as having distinct velocity pulses in much recent researches [9, 14-19]. Moreover, the acceleration time histories of the 1978 Tabas (Tabas station), the 1977 Naghan (Naghan station), the 1990 Rudbar (Abbar station), the 1998 Golbaft (Sirch station) and the 2003 Bam (Bam Station) Iranian near-fault pulse like earthquakes were added to this database. Records were taken from PEER strong motion data base and Iran strong motion network data bank [20, 21]. All ground motions have been recorded on stiff and very dense soil and rock based on the standard No. 2800 site classes for all faulting styles. The earthquake magnitude, M_w, ranges from 6.2 to 7.2, and the closest distance to fault rupture ranges from 0.07 to 18.2 km.

Considering that near-fault ground motions have orientations controlled by the geometry of the fault, specifically by the strike, dip, and rate angle (direction of slip) on the fault, treating them as a vector rather than scalar quantities becomes necessity. The simplest method to treat them as vector quantities is to partition them into fault-normal and fault-parallel components [22]. Accordingly, in this study, 40 near-fault ground motion records have been archived in the fault-normal and fault-parallel components using the transformation method proposed by Somerville [22]. It should be noted that for Iranian near-fault records excluding the 2003 Bam record, there is not any knowledge about their recording orientation. The amount of recording orientation for the aforementioned Iranian earthquake records has been assumed in such a way that the peak of the corresponding displacement response spectra due to their normal components achieves the maximum value. The resulting velocity spectra of the fault-normal and fault-parallel components for the Iranian near-fault earthquakes are provided in Figure 1. This figure confirmed that ground motions in near-fault are strongly influenced by orientation effects such that the fault-normal component is much more severe than the fault-parallel component. From this figure it can be seen that at least one predominant peak can be clearly observed in the velocity response spectra of the fault-normal components. In a study reported by Krawinkler and coworker [24] has been shown that the period of the pulse contained in a near-fault record can be estimated from the predominant peak of its fault-normal velocity spectrum. Pulse periods which is a function of magnitude, distance and fault mechanism [12] for the Tabas, the Naghan, the Rudbar, the Golbaft and the Bam earthquakes are respectively equal to 4.69, 0.66, 2.66, 1.23 and 1.68 seconds. As a consequence of pulse motions effects pseudo spectral accelerations of each record increment in the range around its pulse period [24] having different value in different earthquake records, and thereby median spectrum cannot represent this unusual characteristic of near-fault records adequately. The mean and mean plus or minus the standard deviation of Iranian near-fault earthquake records for fault-normal and fault-parallel components are shown in Figure 2. This figure shows that the median response spectrum of the fault-normal spectra is greater than the fault-parallel spectra; however, the great deal of information about the incrementing in spectral ordinates around the pulse periods in different records is inevitably lost when calculating the mean response spectrum. Large amount of variability in the fault-normal spectra compared to the fault-parallel spectra confirms that spectral ordinates of the fault-normal component increase around the different pulse period in deferent records.

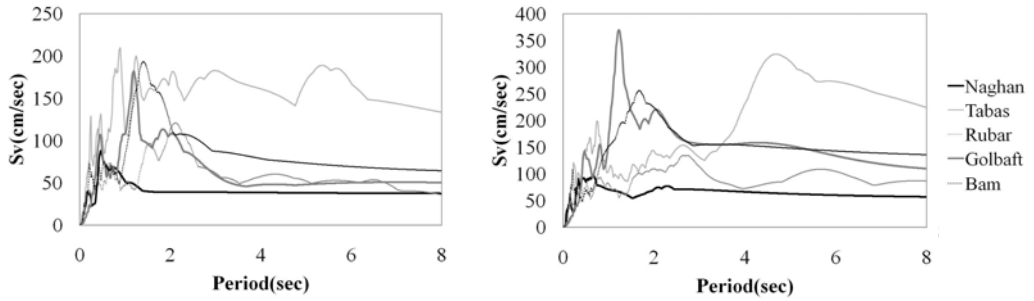

(a) fault-parallel component (b) fault-normal component

Figure 1. Velocity spectra of fault-normal and fault-parallel component for Iranian near-fault earthquake records

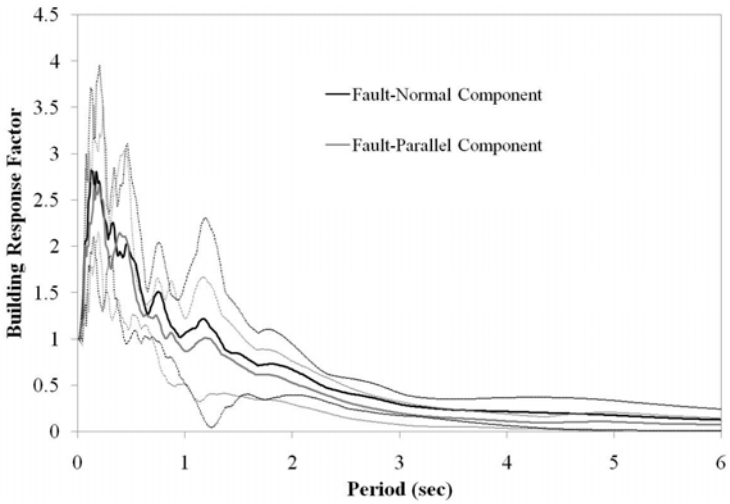

Figure 2. Mean and mean plus or minus standard deviation of building response factor for Iranian near-fault earthquake records

Regarding the more severity of the fault-normal component and the results of a study performed by Krawinkler and Alavi showing that when a structure composed of frames in two perpendicular directions is subjected to a near-fault ground motion, frames in one of the two directions will be subjected to excitations almost as severe as the fault-normal component [25], the efficiency of the scaling methods is evaluated by using the fault-normal components of near-fault ground motions in this study.

3. STRUCTURAL SYSTEMS

Considering the objective of this study, developing the appropriate scaling method for near-

fault earthquake ground motions in such a way that it leads to small scatter in the dynamic responses of structures at different levels of intensity, conducting incremental dynamic analysis (IDA) for structural systems which do not represent a specific structure, becomes inevitability. For this purpose, regular frames are modeled by using two-dimensional generic one-bay frames proposed by Medina and Krawinkler [26] for which the sensitivity of results to different stiffness properties can be readily evaluated.

The generic frames used in this study consist of frames with number of stories, N, equal to 3, 6, 9, 12, 15 and fundamental periods, T_1, of 0.1N. These frames are modeled using the open system for earthquake engineering simulation [27]. The main characteristics of these models are as follow [26];

- The frames are two dimensional.
- The same mass is used at all floor levels.
- They have constant storey height equal to 3.66m (12′) and beam span equal to 7.32m (24′).
- The same moment of inertia is assigned to the columns in a storey and the beam above them.
- Relative stiffnesses are tuned so that the first mode is a straight line (a spring is added at the bottom of the first-storey columns to achieve a uniform distribution of moments of inertia over the height).
- Absolute stiffnesses of beams and columns are tuned such that $T_1 = 0.1N$.
- Frames are designed so that simultaneous yielding is attained under a parabolic (NEHRP, k=2) load pattern.
- Global (structure) P-delta is included.
- Axial deformations and M-P-V interaction are not considered.
- For the nonlinear time history analyses, 5% Rayleigh damping is assigned to the first mode and the mode at which the cumulative mass participation exceeds 95%.

Plastification is modeled by using rotational spring at the beam ends and at the bottom of the first-storey columns. Peak oriented hysteretic model is used to represent the nonlinear behavior of these springs. Since, under cyclic behavior, several system parameters may deteriorate after each excursion, the deterioration model proposed by Ibara and Krawinkler [28] is used in this study to consider the four sources of cyclic deterioration, basic strength, post-capping strength, unloading stiffness, and accelerated reloading stiffness by utilizing energy based deterioration through a cyclic deterioration parameters, $\gamma_{s,c,k,a}$.

It should be noted that the structural demand parameter considered in this study is the peak maximum interstory drift ratio (IDR_{max} , peak response over time and maximum over the height of the structures) because IDR_{max} correlates well with the structural and nonstructural damage of structures.

4. EVALUATING THE EFFICIENCY OF DIFFERENT SCALING METHODS

The seismic demands of a structure at any intended level of intensity can be estimated from nonlinear time history analyses under a suitable set of earthquake records scaled using an appropriate seismic scaling index. It is obvious that the amounts of seismic demands determined from the structural analyses under an ensemble of scaled earthquake records are

randomly different and vary from one tremor to another. Considering the importance of reducing the dispersions the scaling parameter, which has to describe the damage potential of input strong motions, plays the vital role in reliable estimation of the seismic demands of structures.

To reduce the dispersions in the seismic demands of structures under near-fault ground motions, the efficiency of PGA, EPA, IEPA, EPV, IEPV and $S_a(T_1)$ as the scaling indexes are evaluated in order to develop the improved scaling method based on the strengths and weaknesses of these scaling parameters. Peak value of the acceleration time history of ground motions (PGA) is the simplest acceleration-related intensity parameter, which is most commonly applied in earthquake engineering [10], and on which the scaling method in current Iranian seismic design provisions is based. Effective peak acceleration (EPA) and effective peak velocity are two scaling parameters used in the early versions of U.S. codes and guidelines ATC-3 [29]. EPA is equal to the mean value of pseudo spectral accelerations over the period range of [0.1s, 0.5s] divided by an empirical factor 2.5. EPV in accordance with the Kurama and Farrow suggestion is calculated as the mean spectral velocity for the period range of [0.8s, 1.2s] divided by factor 2.5 [30];

$$EPA = S_a(0.1s, 0.5s)/2.5 \quad , \quad EPV = S_v(0.8s, 1.2s)/2.5 \tag{1}$$

EPA and EPV describe the intensity of input records in terms of the spectral ordinates over the fixed period range without much explicit regard to the different frequency contents of near-fault and far-fault ground motions. Actually, in near-fault motions the periods where the pseudo spectral acceleration and spectral velocity reach maxima (denoted as T_{PA} and T_{PV} correspondingly) are generally larger than the respective period of far-fault motions. Based on this fact Yang and coworker [10] proposed the improved effective peak acceleration, IEPA, and improved effective peak velocity, IEPV, for near-fault ground motions as follows:

$$IEPA = \frac{S_a(T_{PA} - 0.2s, T_{PA} + 0.2s)}{2.5}, \quad \text{IEPV} = \frac{\mathrm{S_v}(T_{PV} - 0.2s, \mathrm{T_{PV}} + 0.2s)}{2.5} \tag{2}$$

Figure 3 presents the cumulative distribution of the ratio of EPA, IEPA, EPV and IEPV to PGA for the fault-normal components of ground motions records used in this study. This figure implies that these ratios for records used in this study can be well-fitted with the lognormal distribution. From this figure it can be seen that IEPA compared to EPA is more close to PGA and the ratio IEPV/PGA varies in relatively wide range of [0.05, 0.33s] compared to EPV/PGA varying in the range of [0.03, 0.17s] due to pulse effects in near-fault records.

For each of the parameters PGA, EPA, IEPA, EPV, IEPV and $S_a(T_1)$ as the seismic intensity Index, the associated intensity of each record leading to immediate occupancy (IO), life safety (LS) and collapse (CP) levels are computed as the intensity at IO, LS and CP respectively for each frame. Regarding the Incremental Dynamic Analyses results the measure of intensity of each record that imposes the IDR_{max} equal to 0.25 and 2.0 times the yield interstory drift ratio are referred to as the intensity at IO and LS respectively for each frame. The intensity at which the IDR_{max} demand is equal to 4.0 times the yield interstory

drift ratio or the nonlinear dynamic analysis does not converge is defined as the intensity at CP for each frame.

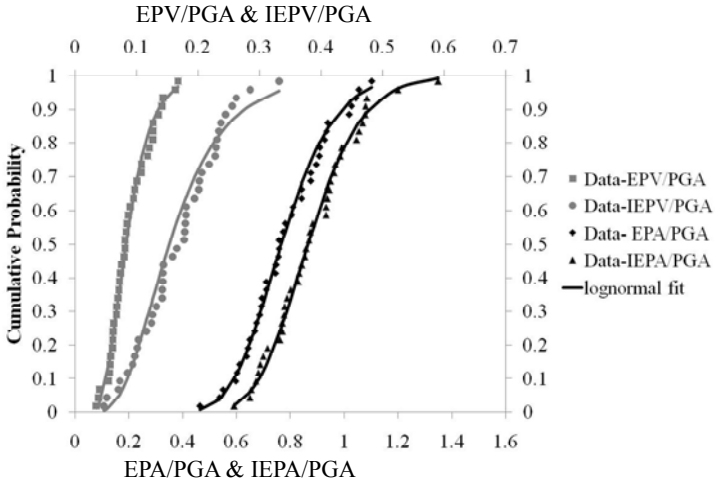

Figure 3. Cumulative distribution of the ratio of EPA, IEPA, EPV and IEPV to PGA for the fault-normal components of ground motions records used in this study

To provide quantitative criteria for comparing the efficiency of these Intensity measures, IMs, the mean values and the coefficient of variation (COV) of associated intensities with the aforementioned performance levels, denoted as $\overline{IM}$ and $(COV)_{IM}$ respectively, are computed by the following equations for each of the scaling parameters:

$$\overline{IM} = \sum_{1}^{n} IM_i / n \tag{3}$$

$$(COV)_{IM} = \frac{1}{\overline{IM}} \left[\sum_{1}^{n} (IM_i - \overline{IM})^2 \Big/ (n-1) \right]^{1/2} \tag{4}$$

Where IM_i is the intensity of ith record at which the desired performance levels was exceeded and n is the total sample of observations (total sample of records which is equal to 40 in this study).

Figures 4a, 4b and 4c present the $(COV)_{IM}$ of the records intensities at the IO, LS and CP levels respectively for the cases where the intensity of records are estimated by PGA, EPA, IEPA, EPV, IEPV and $S_a(T_1)$. Figure 4 shows that $S_a(T_1)$ generally predicts the IDR_{max} of frames better than other considered scaling parameters, however it can be seen that the efficiency of $S_a(T_1)$ reduces as the number of stories or the level of intensity increase as a result of higher modes and period elongation effects. From comparing the efficiency of PGA, EPA, IEPA, EPV, IEPV detailed observation is given as follow:

- At the IO and LS performance levels, for 3 and 6 storey frames EPA and IEPA respectively and for 9 , 12 and 15 storey frames EPV lead to the result with less variations.

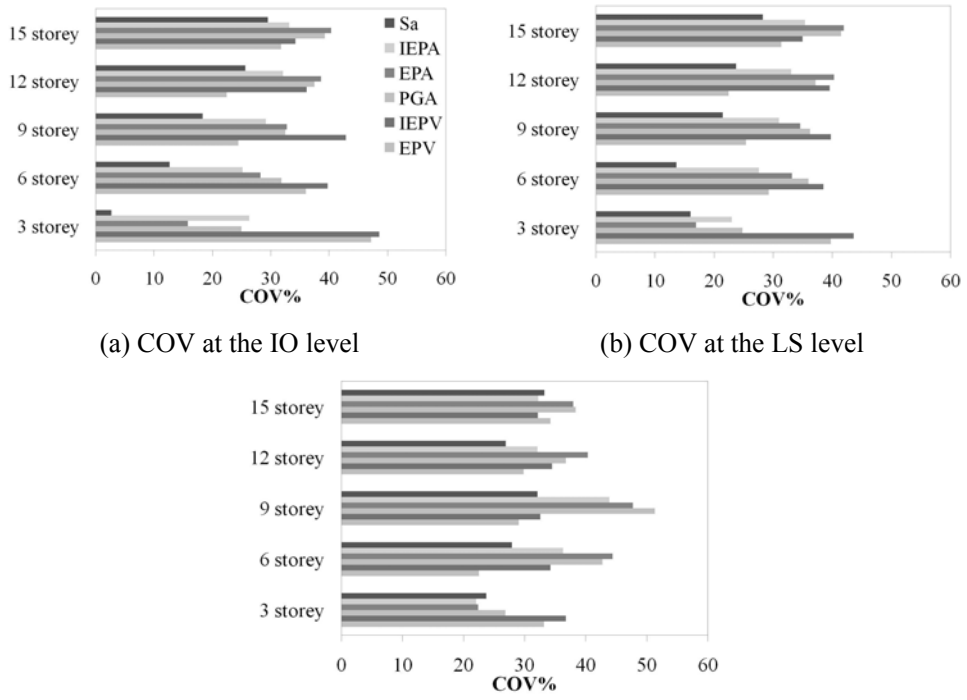

(a) COV at the IO level

(b) COV at the LS level

(c) COV at the CP level

Figure 4. COV in IDR_{max} at a) Immediate Occupancy b) Life Safety, C) Collapse levels for 3, 6, 9, 12 and 15 story generic frames

- At the CP level at which the frames respond more inelastically, for 3 storey frame IEPA and for 6, 9, 12 storey frames EPV and for 15 storey frame IEPV lead to the result with less variations even with respect to those of $S_a(T_1)$ except for 12 storey frame.
- The acceleration-related indices (EPA and IEPA) and the velocity-related indices (EPV and IEPV) are respectively correlated with the demand parameters in frames with short-period and medium to long period regarding the period elongation effect. As an instance, for 6 storey frame at the performance levels of IO and LS, IEPA presents the best correlation, however at the CP levels due to softening EPV presents the best correlation with the seismic demands.
- Using PGA as the scaling parameters leads to the result with a large COV which varies up to 52 percent at the CP level for 9 storey frame. This parameter which is used in standard No. 2800 of Iran as the seismic intensity scaling index is not superior to EPA in short period structures and EPV in medium to long period structures at all performance levels.
- IEPA and IEPV which respectively estimate the intensity of each record based on the its average spectral ordinates around the predominant period of acceleration and velocity response spectrum disregarding the vibrations periods of structures cannot generally enhance the performance of scaling parameter of conventional parameters, i.e. EPA and

EPV. This is because EPA and EPV represent the intensity of each record based on its average spectral ordinates over the fixed period range of [0.1s, 0.5s] and [0.8s, 1.2s] respectively and thereby can predict the seismic demands of a structure fairly good in the cases where the effective periods of vibrations of the structure considering the period elongation effects are within these fixed period range.

5. IMPROVEMENT OF THE SEISMIC INTENSITY SCALING METHOD

Inspection of the variations in the results at different intensity levels and different number of stories for aforementioned scaling parameters presented in section 4 reveals that using pseudo spectral acceleration at the main period of structures can be responsible for the damage potential of input records as long as higher mode effects and also period elongation effects don't dominate the response of structures. However, when the input time history is a near-fault pulse with the pulse period in the range of the periods of effective mode of vibrations, these effects are accentuated to the point that spectral ordinates increment around the pulse period. Results also show that EPA and EPV describing the intensity of records based on the average spectral response over the fixed range of [0.1, 0.5] and [0.8, 1.2] respectively have relatively good correlation with the response of a structures providing its effective periods are in these specified fixed range.

Considering the abovementioned issues, the improved index could be superior to these parameters on condition that containing more information about the spectral responses at effective period range of structures regarding the effects of higher modes and period elongation due to nonlinear behavior of structures. Due to this matter, root-mean-square value of pseudo spectral acceleration, $(S_a)_{rms}$, may be used as the improved scaling parameter to reduce the scatter in the dynamic responses. The efficiency of the root-mean-square value depends on using proper effective period range, because without recognition of the spectral values that affect the structural responses, dispersions would not be reduced.

Range of effective periods of vibrations has been determined with regards these two points of view. First, regarding the higher mode effects on the dynamic responses, the scaling parameter should represent spectral responses in higher modes of vibration. Second, to scale ground motions to different intensity levels, effective period range should be defined in such a way that it can reduce the variations of the dynamic responses at all intensity levels (corresponding to different demand ductility levels). In order to reach the first goal, the effective elastic period range of $[T_m\,,\ T_1]$ has been defined in which T_1 and T_m are period of the first mode and the mode at which the cumulative mass participation exceeds 95%, respectively. Accordingly in order to reach the second goal, regarding the fact that structural periods increase because of nonlinear behavior, the range of effective elastic period could be multiplied by a modification coefficient of $C_T(\mu)$. It is well known that the period of structure is reversely related to root of structural secant stiffness. On the other hand, secant stiffness (at ductility level of μ) considering the hardening ratio,α_s, is equal to product of $\sqrt{(\alpha_s\mu+1-\alpha_s)/\mu}$ and elastic stiffness [30]. Hence at the ductility level of μ the period T_μ is approximately equivalent to the product of elastic period and

$C_T(\mu) = \sqrt{\mu/(\alpha_s \mu + 1 - \alpha_s)}$. Therefore, the effective period range of structure at ductility level of μ is assumed to be in the range of $[C_T(\mu)T_m, C_T(\mu)T_1]$.

As in IDA the mean ductility demand depends on the intensity level of input ground motions, the period range of effective modes of vibration is not the same and it is a function of earthquake intensity level. Therefore, the period range of effective modes cannot be defined in such a way that the efficiency of the scaling parameter to be in the best situation at all intensity levels. In this study, with the aim of unification of diversity at all levels of intensities and minimizing it, the efficiency of period ranges of $[1.9T_m, 1.9T_1]$, $[T_m, 1.9T_1]$ and $[1.5T_m, 1.5T_1]$ have been examined and compared. These period ranges, which will be denoted from here on as the period range *No.1* ,*No.2* and *No.3* respectively, are determined by multiplying the high and low limits of $[T_m, T_1]$ with the maximum and the average value of $C_T(\mu)$ which represent the amount of period elongation due to softening. Period range *No.1* which represents the period range at the median ductility level equal to ductility capacity of frames (μ_c=4) is evaluated because most variations are usually between performance levels of life safety and fully collapse at which structures respond more inelastically. The efficiency of period range *No.2* is considered in order to stipulate whether the higher mode effects in linear region dominate the response. Period range *No. 3* is defined in order to consider the efficiency of the period range that represents the intermediate state of softening.

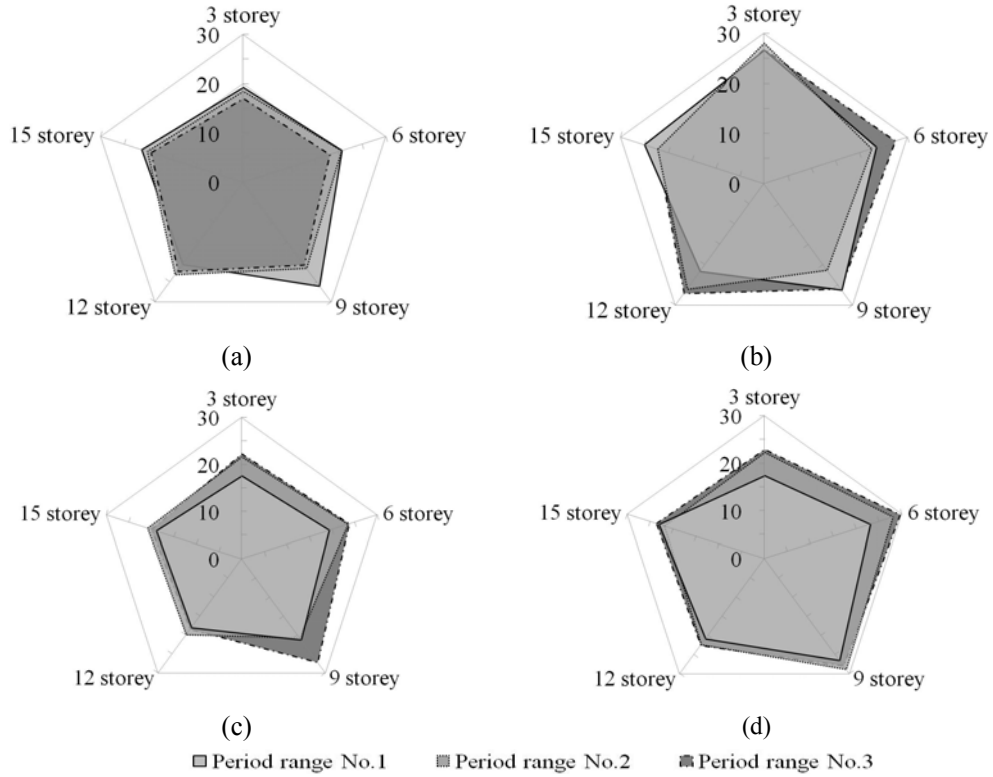

Figure 5. COVs in IDR_{max} at median ductilty demand of (a) 1, (b) 2, (c) 3, (d) 4 for $(S_a)_{rms}$ over different period ranges

For each of three abovementioned period ranges, $(S_a)_{rms}$ has been computed as the parameters described the intensity of records, then the results of IDA for generic frames of 3, 6, 9, 12 and 15 storey under 40 records have been studied and the variations of the dynamic responses at different levels of $(S_a)_{rms}$ (for each of three abovementioned period ranges) have been computed. The variations of the dynamic responses at some levels of $(S_a)_{rms}$ at which the average demand of the peak maximum interstory drift ratio corresponds with ductility levels of 1, 2, 3 and 4 are presented in Figure 5. Based on Figure 5, it can be concluded that although application of period intervals No.2 and No.3 lead to insignificant less variation in lower levels of ductility in comparison with interval No.1, but this reduction is accompanied with the increase in variations with high intensity in other levels of ductility. This is because the computation of $(S_a)_{rms}$ over period intervals No.2 and 3 comparing to No.1 would lead to the fact that more contribution for spectral responses in linear region is taken into estimating the intensity of an earthquake record. However, considering the variations in the dynamic responses at all ductility levels and all frames, it can be concluded that the period interval No.1, comparing the other two considered intervals has led to the results with less variations on average and thereby is selected as the effective period range for computation of $(S_a)_{rms}$.

6. VARIABILITY REDUCTION IN SEIMIC DEMANDS USING $(S_A)_{RMS}$

Root-mean-square value of pseudo spectral accelerations over the effective period range of structures, $(S_a)_{rms}$, representing the higher mode and period elongation effects, can enhance the performance of scaling parameter of $S_a(T_1)$. To provide the evidence for this statement results of the incremental dynamic analyses of 3 and 15 generic frames are presented by plotting the scaled intensity measure versus IDR_{max} in Figure 6 as examples. Each curve is collection of the results determined from the nonlinear time history analyses, under a single record scaled to multiple intensity levels. Results are plotted for 3 and 15 storey frames in terms of the $S_a(T_1)$ in Figures 6a and 6b and in terms of the $(S_a)_{rms}$ in Figures 6c and 6d respectively. Graphs in Figures 6a and 6c reveal that for 3 storey frame $S_a(T_1)$ provides a nearly exact correlation with the linear responses at lower levels of intensity, whereas the $(S_a)_{rms}$ works well when the structure behaves nonlinear at higher levels of intensity. From this figure it can be seen that using $(S_a)_{rms}$ instead of $S_a(T_1)$ improves the R-squared value from 0.419 to 0.505 at high intensity levels, however the R-square value is slightly decrease from 0.998 to0.993 at low levels of intensity. Comparing the graphs in Figures 6b and 6d, it is obvious that for 15 storey generic frames the $(S_a)_{rms}$ results in significantly less variability compared to $S_a(T_1)$ at all levels of intensity and improves the R-squared value from 0.863 to 0.916 at low levels of intensity and from 0.644 to 0.775 at high levels of intensity.

The coefficients of variations in the seismic demands of generic frames determined from nonlinear dynamic analyses under 40 near-fault pulse-like records at different levels of intensity based on $(S_a)_{rms}$ and $S_a(T_1)$ as the scaling parameter provide in Figure 7. In this figure the ordinate and abscissa respectively represent the estimated median value and the coefficient of variations in the ductility seismic demands at different intensity levels. From this figure it can be seen that for $(S_a)_{rms}$ the variations are nearly independent of the level of

ductility demand and the number of stories and range from 16.5% to 28.9%. Whereas, the variations for $S_a(T_1)$ are strictly dependent on the number of stories and the level of intensity. Based on $S_a(T_1)$ criterion, the variations are in the wide range up to as high as 49.5%.

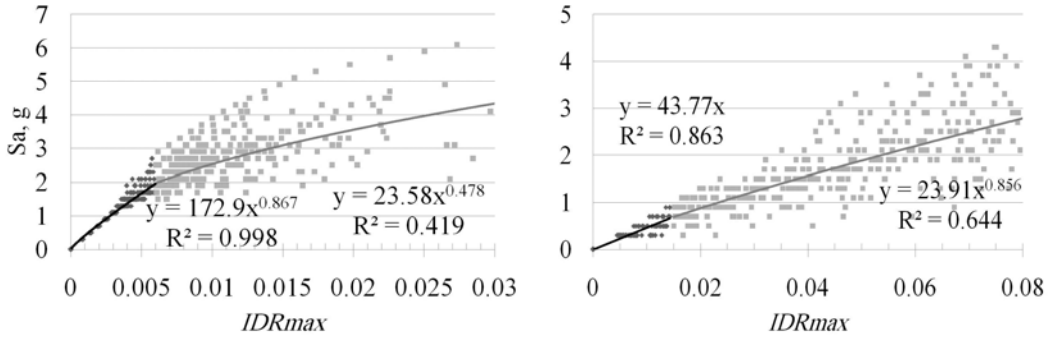

(a) IDA results of 3 storey frame

(b) IDA results of 15 storey frame

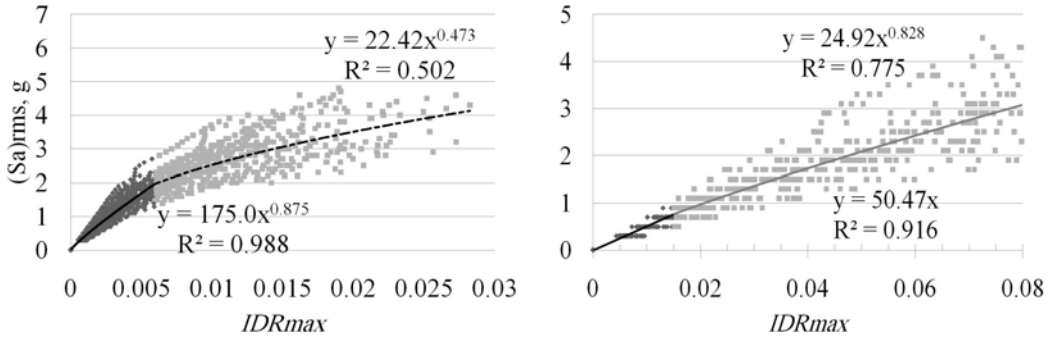

(c) IDA results of 3 storey frame

(d) IDA results of 15 storey frame

Figure 6. IDA results based on $S_a(T_1)$ and $(S_a)_{rms}$ as the scaling parameter

In 3, 6 and 9 storey frames and at low levels of ductility demand (i.e. median ductility demand less than 2.5), using the $S_a(T_1)$ compared to $(S_a)_{rms}$ leads to the results with less variations. Nevertheless, by increasing the number of stories from 3 to 6 and 9, the difference between efficiency of $S_a(T_1)$ and $(S_a)_{rms}$ is decreased, since the effects of higher modes in estimating the structural response would gain more significance.

In 3, 6 and 9 storey frames, an increase in ductility demand level which means increase in structural period because of nonlinear behavior, $S_a(T_1)$ criterion comparing with $(S_a)_{rms}$ cannot predict the structural responses adequately. Consequently the variations of the dynamic responses are increased according to this scaling parameter which can reduce by using $(S_a)_{rms}$. For example at ductility level of 4, the scaling parameter of $(S_a)_{rms}$ reduces the variations in dynamic response of 3, 6 and 9 storey frames with the ratio of 26, 17 and 17 percent respectively relative to those of $S_a(T_1)$.

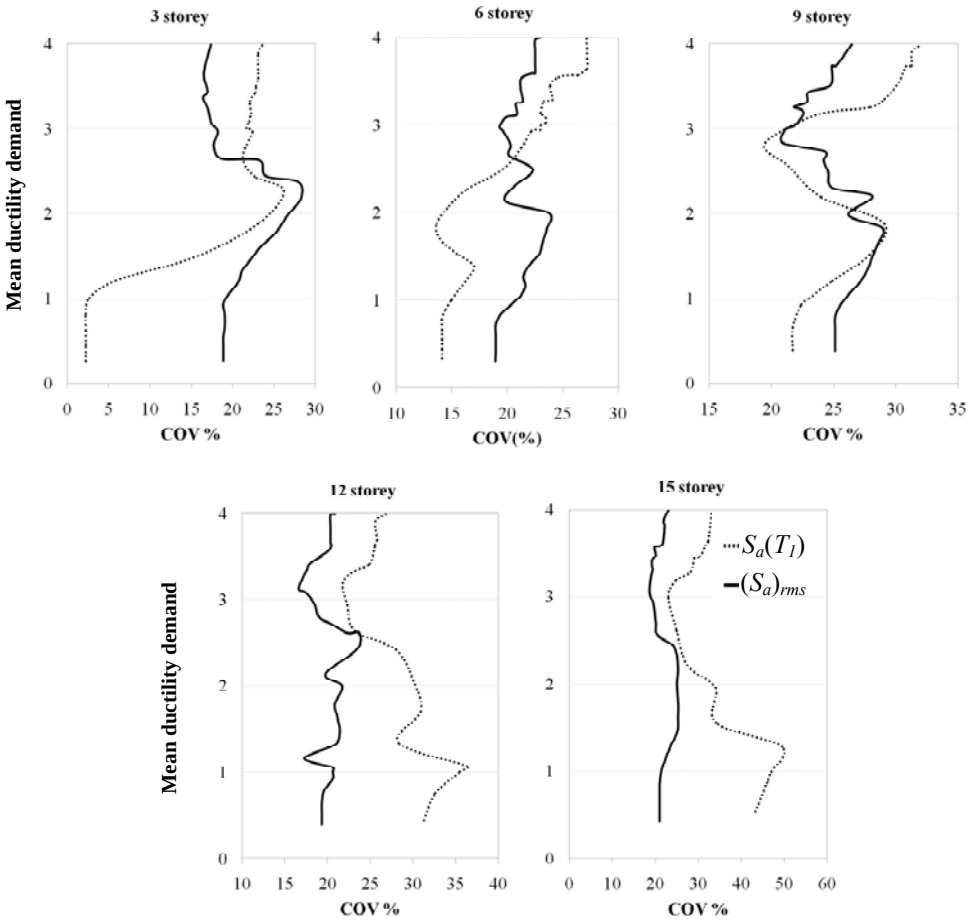

Figure 7. The coefficients of variations in the peak maximum interstory drift ratio at different ductility levels for 3, 6, 9, 12 and 15 storey generic frames

In 12 and 15 storey frames, because of the importance of higher mode effects and as the pulse periods of near-fault records are usually in the effective periods of these structures, $(S_a)_{rms}$ considerably reduces the variability at all ductility levels.

Considering the results which are shown in Figure 7 and the abovementioned issue $(S_a)_{rms}$ has the minimum changes in the variations of the dynamic responses in different frames and different ductility levels, and since the variations in the dynamic responses is less than $S_a(T_1)$ on average, scaling the input records based on this parameter can improve the level of confidence to the estimated mean value of interested seismic demands.

7. CONLCLUSIONS

In this study with the objective of reducing the variability in the maximum interstorey drift

ratios of generic frames of 3, 6, 9, 12 and 15 storey under near-fault pulse-like ground motions, the new scaling parameter has been developed. For this purpose, the efficiency of Peak Ground Acceleration, PGA, Effective Peak Acceleration, EPA, Effective Peak Velocity, EPV, Improved Effective Peak Acceleration, IEPA, Improved Effective Peak Velocity, IEPV and spectral acceleration measured at the first mode, $S_a(T_1)$, has been studied to develop the improved scaling parameter based on the weakness and strength points of these seismic scaling parameters. The overall conclusions of this study are as follow:

1. PGA used in the standard No. 2800 of Iran as the seismic intensity scaling index introduces a large scatter up to 52 percent in the seismic demands obtained from nonlinear dynamic analyses of structures compared to other considered scaling parameters for different number of stories and different intensity levels.
2. IEPA and IEPV cannot enhance the performance of EPA and EPV as the scaling parameter; because the period ranges over which IEPA and IEPV are calculated are defined respectively around the predominant period of pseudo acceleration and velocity spectra of each input record. Whereas large value of the spectral responses are considered as damage potential for a structure only if happening around the vibrations periods of the structure.
3. EPA and EPV have fairly good correlation with the response of a structure in the cases where the effective vibration periods of the structure is within the period range of [0.1, 0.5] and [0.8, 1.2] respectively. Effective vibration periods of a structure vary with the intensity level of input ground motions due to period elongation effects.
4. $S_a(T_1)$ don't introduce a large variability in the seismic demands as long as higher mode effects and period elongation effects don't dominate the response of a structure. It is worth noting that when the input time history is a near-fault pulse with the pulse period in the range of the vibrations periods of a structure, these effects are accentuated to the point that spectral ordinates increment around the pulse period.
5. Root-mean-square value of pseudo spectral accelerations, $(S_a)_{rms}$, calculated over the effective periods of a structure could be responsible for damage potential of input ground motions records because it represents enough information about the effective spectral responses. To recognize the effective periods of vibrations of a structure, three period ranges for computation of $(S_a)_{rms}$ regarding the period elongation amount due to softening have been evaluated. The results show that the application of period range of $[1.9T_m\ ,1.9T_1]$, the period range of modes which cover 95% of structural mass in linear region and has been modified for increasing the period of structure because of nonlinear behavior, considering the variations in the dynamic responses at all ductility levels and all frames comparing to the other two considered intervals**,** $[T_m\ ,1.9T_1]$ and $[1.5T_m, 1.5T_1]$, lead to results with less variations on average for the structure with the ductility capacity of 4.
6. Application of $(S_a)_{rms}$ compared to $S_a(T_1)$ as scaling parameter can reduce the variations in the dynamical responses resulted from time history analyses at different levels of ductility for 12 and 15 storey frames. Applying $(S_a)_{rms}$ in dynamic analyses of these frames has reduced the variations of structural drifts at different ductility demand levels to the amount of 25 and 35 percent relative to those of $S_a(T_1)$ on average. This scaling parameter can also reduce the variations of structural drifts in 3, 6 and 9 storey frames at

higher levels of ductility demand.

7. By using of $(S_a)_{rms}$, it is resulted that the variations in the structural responses and consequently standard error of the estimated mean demand is nearly independent from ductility demand level (elastic to fully collapse levels) and the number of stories. Based on $(S_a)_{rms}$, the coefficient of variations ranges from 16 to 29 percent. Meanwhile the scaling ground motions based on $S_a(T_1)$, results in such a way that the coefficient of variations strictly depend on the number of stories and ductility levels. It was seen that in the case of using of $S_a(T_1)$ the coefficient of variations vary up to 50 percent.

REFERENCES

1. Bozorgnia Y, Bertero VV. *Earthquake Engineering from Engineering Seismology to Performance-Based Engineering,* CRC Press, 2004.
2. Building and House Research Center, Standard No. 2800: Iranian Code of Practice for Seismic Resistance Design of Buildings, 2007.
3. Shome N, Cornell C. Normalizing and scaling accelerograms for nonlinear structural analysis, *Proceeding of the Sixth U.S. National Conference on Earthquake Engineering*, Seattle, WA, 1998.
4. Miranda E. Site-dependent strength-reduction factors, *Journal of Structural Engineering ASCE*, **119**(1993) 3503-19.
5. Benjamin JR, Cornell CA. *Probability, Statistics, and Decision for Civil Engineers*, McGraw Hill, Inc. New York, 1970.
6. Shome N, Cornell C, Bazzurro P, Carallo J. Earthquakes, records, and nonlinear responses. *Earthquake Spectra* **14**(1998) 469-500.
7. Galesorkhi R, Gouchon J. Near source effects and correlation to recent recorded data, *Proceedings of the 6th U.S. National Conference on Earthquake Engineering*, Seatle, Wah, 2000.
8. KalKan E, Kunnath SK. Effects of fling steps and forward directivity on seismic response of buildings, *Earthquake Spectra*, No. 2, **22**(2006) 367-90.
9. Tothong P, Luco N. Probabilistic seismic demand analysis using advanced ground motion intensity measures, *Earthquake Engineering & Structural Dynamics*, No. 13, **36**(2007)1837-60.
10. Yang D, Pan J, Li G. Non-structure-specific intensity measures parameters and characteristics of near-fault ground motions, *Earthquake Engineering & Structural Dynamics*, **38**(2009) 1257-80.
11. Somerville P, Smith N, Graves R, Abrahamson N. Modification of empirical strong motion attenuation relations to include the amplitude and duration effects of rupture directivity, *Seismological Research Letters,* **68**(1997a) 199-222.
12. Stewart JP, Chiou S, Bray JD, Graves RW, Somerville PG, Abrahamson NA. Ground motions evaluation procedures for performance based-design, Report 2001/09, PEER, Berkeley, CA, 2001.
13. Abrahamson N. Incorporation effects of near fault tectonic deformation into design ground motions, *A presentation sponsored by the Earthquake Engineering Research*

Institute Visiting Professional Program, hosted by State University of New York at Buffalo, 2001.
14. Krawinkler H, Alavi B. Development of improved design procedures for near fault ground motions, *Proceedings of the SMIP98, Seminar on Utilization of Strong Motion Data*, Oakland, Calif. 1998.
15. Somerville PG, Development of an improved representation of near fault ground motions, *Proceeding of the SMIP98 Seminar on Utilization of Strong Motion Data*, California Strong Motion Instrumentation Program, Sacramento, CA, 1998.
16. Chopra AK, Chintanapakdee C. Comparing response of SDF systems to near-fault earthquake motions in the context of spectral regions, *Earthquake Engineering & Structural Dynamics,* **30** (2001) 1769-80.
17. Mavroeidis GP, Papageorgiou AS. A mathematical presentation of near-fault ground motions, *Bulletin of the Seismological Society of America*, No. 3 , **93**(2003)1099-1131.
18. Bray JD, Rodriguez-Marek A. Characterization of forward-directivity ground motions in the near-fault region, *Soil Dynamics and Earthquake Engineering*, **24**(2004) 815-28.
19. Loh Ch, Wan S. Earthquake response of RC moment frames subjected to near-fault ground motions, *Bulletin of the Seismological Society of America,* **93**(2004) 1099-1131.
20. PEER Strong Ground Motion Database, http://peer.berkeley.edu/smcat/
21. Iran Strong Motion Network Data Bank, http://www.bhrc.ac.ir
22. Somerville PG. Characterizing near fault ground motion for the design and evaluation of bridges, *Proceedings of the Third National Seismic Conference and Workshop on Bridges and Highways,* Portland, Oregon, 2002.
23. Krawinkler H, Alavi B, Zareian F. Impact of near-fault pulses on engineering design, *Direction in Strong Motion Instrumentation,* **58(**2005) 83-106.
24. Chioccarelli E, Iervolino I. Near-source seismic demand and pulse-like records: A discussion for L Aquila earthquake, *Earthquake Engineering & Structural Dynamics,* No. 9, **39**(2010)1039 - 62
25. Krawinkler H, Alavi B. Seismic drift and ductility demands and their dependence on ground motions, *Eng. Struct.*, **25**(2004) 637-53.
26. Medina R, Krawinkler H. Seismic Demands for Nondeteriorating Frame Structures and Their Dependence on Ground Motions, *Report No. PEER 2003/15*, Pacific Earthquake Engineering Research Center, University of California at Berkeley, Berkeley, CA, 2004.
27. OpenSees, Open System For Earthquake Engineering Simulation, *Pacific Earthquake Engineering Research Center*, http://peer.berkeley.edu/, 2009.
28. Ibarra LF, Krawinkler H. Global collapse of frame structures under seismic excitations, John A. Blume Earthquake Engineering Center, Report No.152, Department of Civil and Environmental Engineering, Stanford University, Stanford, CA, 2005.
29. Applied Technology Council. Tentative provisions for the development of seismic regulations for buildings, *Report No. ATC 3-06*, Palo Alto, CA, 1978.
30. Kurama YC, Farrow KT. Ground motion scaling methods for different site conditions and structure characteristics, *Earthquake Engineering & Structural Dynamics,* **32**(2003) 2425-50.